

See discussions, stats, and author profiles for this publication at: <https://www.researchgate.net/publication/233962921>

# Universal Transients in Polymer and Ionic Transition Metal Complex Light-Emitting Electrochemical Cells

ARTICLE in JOURNAL OF THE AMERICAN CHEMICAL SOCIETY · DECEMBER 2012

Impact Factor: 12.11 · DOI: 10.1021/ja3107803 · Source: PubMed

CITATIONS

19

READS

47

5 AUTHORS, INCLUDING:



**Stephan van Reenen**

Technische Universiteit Eindhoven

14 PUBLICATIONS 223 CITATIONS

SEE PROFILE



**Takeo Akatsuka**

Nippon Shokubai

10 PUBLICATIONS 96 CITATIONS

SEE PROFILE



**Daniel Tordera**

Linköping University

36 PUBLICATIONS 561 CITATIONS

SEE PROFILE



**Henk J. Bolink**

University of Valencia

208 PUBLICATIONS 4,905 CITATIONS

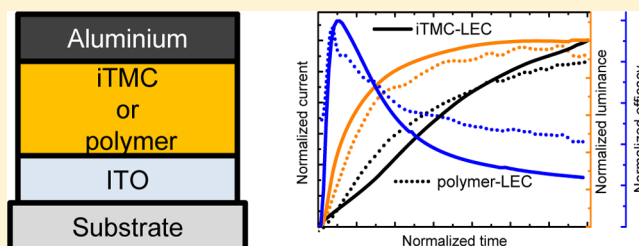
SEE PROFILE

## Universal Transients in Polymer and Ionic Transition Metal Complex Light-Emitting Electrochemical Cells

Stephan van Reenen,<sup>†</sup> Takeo Akatsuka,<sup>‡,§</sup> Daniel Tordera,<sup>‡</sup> Martijn Kemerink,<sup>\*,†</sup> and Henk J. Bolink<sup>\*,‡</sup><sup>†</sup>Department of Applied Physics, Eindhoven University of Technology, P.O. Box 513, 5600 MB, Eindhoven, The Netherlands<sup>‡</sup>Instituto de Ciencia Molecular, Universidad de Valencia, C/Catedrático J. Beltrán 2, ES-46980 Paterna (Valencia), Spain<sup>§</sup>Advanced Materials Research Center, Nippon Shokubai Co., Ltd., 5-8 Nishi Otabi-cho, Suita, Osaka 564-8512, Japan

## Supporting Information

**ABSTRACT:** Two types of light-emitting electrochemical cells (LECs) are commonly distinguished, the polymer-based LEC (p-LEC) and the ionic transition metal complex-based LEC (iTMC-LEC). Apart from marked differences in the active layer constituents, these LEC types typically show operational time scales that can differ by many orders of magnitude at room temperature. Here, we demonstrate that despite these differences p-LECs and iTMC-LECs show current, light output, and efficacy transients that follow a universal shape. Moreover, we conclude that the turn-on time of both LEC types is dominated by the ion conductivity because the turn-on time exhibits the same activation energy as the ion conductivity in the off-state. These results demonstrate that both types of LECs are really two extremes of one class of electroluminescent devices. They also implicate that no fundamental difference exists between charge transport in small molecular weight or polymeric mixed ionic and electronic conductive materials. Additionally, it follows that the ionic conductivity is responsible for the dynamic properties of devices and systems using them. This likely extends to mixed ionic and electronic conductive materials used in organic solar cells and in a variety of biological systems.



## INTRODUCTION

Two decades ago, Pei et al.<sup>1</sup> introduced a polymer light-emitting diode (pLED) admixed with ions, showing attractive properties like a strongly reduced dependence on the active layer thickness and bipolar charge carrier injection from air-stable electrodes, the polymer “light-emitting electrochemical cell” (LEC). A year later, a small molecule alternative was reported using an intrinsically ionic semiconductor: a cationic ruthenium complex from now on referred to as ionic transition metal complex (iTMC).<sup>2,3</sup> For recent reviews of both types of LECs, the reader is referred to Sun et al. and Costa et al.<sup>4,5</sup> The advantages of both types of devices are significant. In general, LECs have a single organic layer that can be deposited from solution. In addition, during operation, carrier transport and injection are enhanced by the ions in the active layer, allowing for low operating voltages and leading to rather good power conversion efficiencies. These features make LECs an interesting type of electroluminescent devices for low-cost large scale production.

The advantage of having a single active layer also proved to be a disadvantage because of its complexity. This is evidenced by a long-standing debate regarding the operational model.<sup>6–8</sup> Recent work however has convincingly identified the operating model that describes both types of cells during steady-state operation.<sup>8–16</sup> According to this model, the salt in the active layer dissociates under the influence of an applied electric field into ions that form electric double layers (EDLs) at the

electrode interfaces. These EDLs enhance the injection of electronic carriers that oxidize or reduce the semiconductor in the active layer. These redox reactions are electrostatically stabilized by the ions, leading to the formation of highly conductive p- and n-doped regions. These two doped regions are separated by an intrinsic or nondoped region where electron–hole recombination and light emission occur. The large carrier density in the doped regions just next to the intrinsic region results in a significant exciton quenching.<sup>12</sup>

Despite the similarity in steady-state operation, large differences exist in key properties such as lifetime, turn-on time, brightness, and efficiency. For comparison, state-of-the-art p-LECs exhibit lifetimes of ~5600 h at a brightness of >100 cd m<sup>-2</sup>.<sup>17–21</sup> iTMC-LECs have similar lifetimes at higher brightness (>600 cd m<sup>-2</sup>).<sup>22,23</sup> Furthermore iTMC-LECs consist of triplet-emitters that intrinsically allow for higher quantum efficiencies. Of all of the key properties, the turn-on time shows the largest difference between both types of devices. Biased at 3–4 V at room temperature, p-LECs typically turn-on within a second, whereas iridium-based iTMC-LECs frequently need hours.<sup>5,9,24–27</sup> These dynamic differences are the main reason that these two types of LECs are considered as different classes.

Here, we report on a comparative study on the transient behavior of stacked LECs based on either the polymer MDMO-

Received: November 1, 2012

Published: December 20, 2012

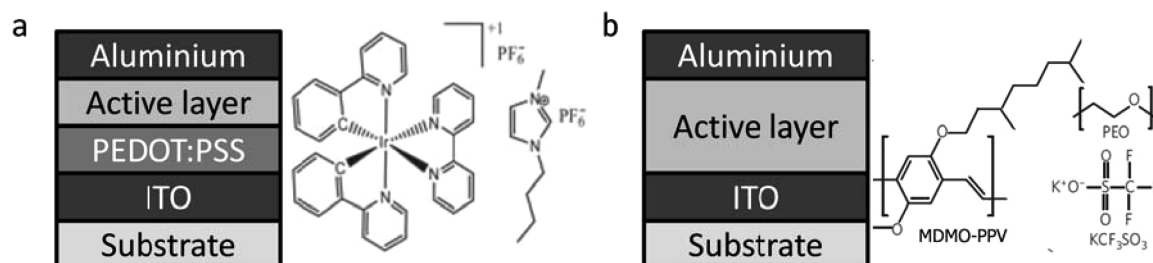


**Figure 1.** Device layout and the structural formulas of the active layer constituents of (a) the iTMC-LEC and (b) the polymer LEC.

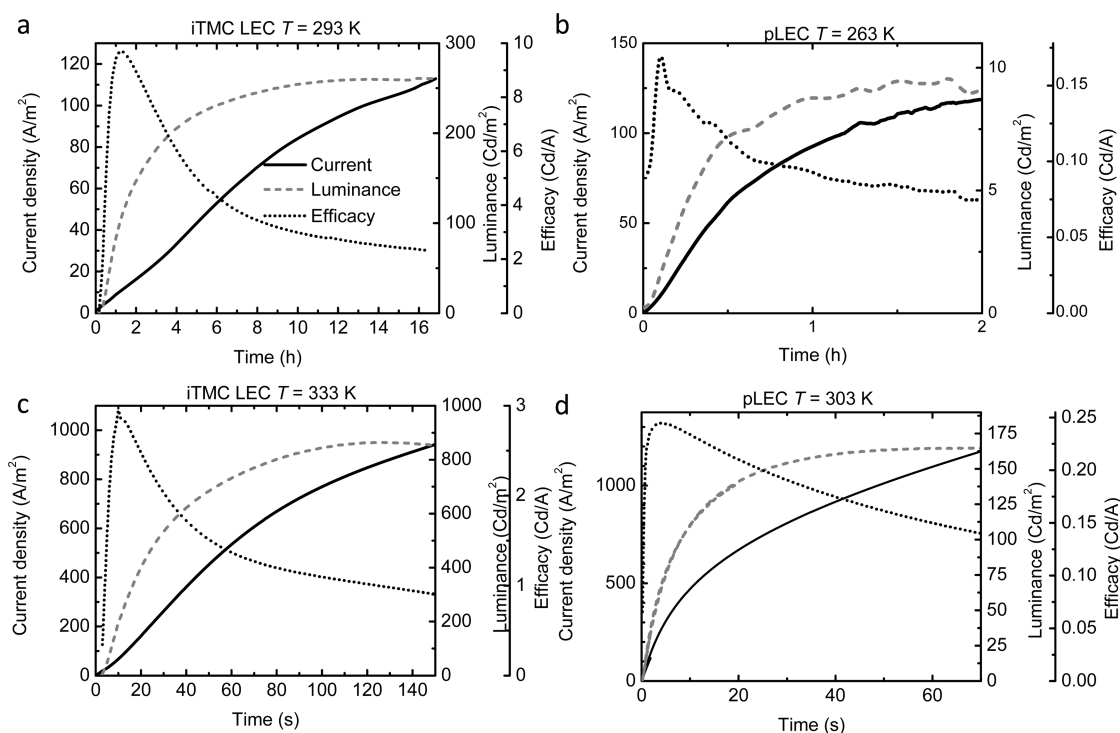


**Figure 2.** Current, luminance, and efficacy transients of (a,c) pristine Ir-iTMC LECs and (b,d) pristine MDMO-PPV LECs biased at 3.5 V. The temperature during operation is shown at the top of each graph.

PPV or the ionic iridium complex bis(2-phenylpyridine)-2,2'-bipyridine-iridium(III) hexafluorophosphate,  $[\text{Ir}(\text{ppy})_2(\text{bpy})]^+ [\text{PF}_6]^-$ . These were studied by determining the current and luminance transients at different cell temperatures. The shape of the transients is found to be independent of operating temperature and more importantly independent of the type of semiconductor used. The turn-on time, however, varied over several orders of magnitude with temperature and could be described by an Arrhenius-type activation energy. The same activation energy was found in the thermal activation of the ion conductivity in the unbiased state: the turn-on time is inversely proportional to the ion conductivity. Together these results prove that next to the steady-state operation, also the transient behaviors of iTMC and polymer LECs are qualitatively the same. Hence, pLECs and iTMC-LECs are really one class of electroluminescent devices. These results also demonstrate that the ionic conductivity is responsible for the dynamic properties of devices and systems using mixed electronic and ionic materials.

## EXPERIMENTAL SECTION

For the conjugated polymer in the active layer of our sandwich LECs, poly[2-methoxy-5-(3',7'-dimethyloctyloxy)-*p*-phenylene vinylene]

(MDMO-PPV,  $M_w > 10^6 \text{ g mol}^{-1}$ , American Dye Source) was used. Poly(ethylene oxide) (PEO,  $M_w = 5 \times 10^5 \text{ g mol}^{-1}$ , Aldrich) was used as received. The salt potassium trifluoromethanesulfonate ( $\text{KCF}_3\text{SO}_3$ , 98%, Aldrich) was dried at a temperature  $T = 473 \text{ K}$  under vacuum before use. MDMO-PPV ( $10 \text{ mg mL}^{-1}$ ) was dissolved in chloroform (>99%, anhydrous, Aldrich). PEO and  $\text{KCF}_3\text{SO}_3$  were dissolved separately ( $10 \text{ mg mL}^{-1}$ ) in cyclohexanone (>99%, anhydrous, Aldrich). These solutions were mixed together in a weight ratio of  $\text{PPV/PEO/KCF}_3\text{SO}_3 = 1:1.35:0.25$ . This stock solution was thereafter stirred on a magnetic hot plate at  $T = 323 \text{ K}$  for 5 h.

Cleaned glass/ITO substrates were spin-coated with the stock solution (at 800 rpm for 60 s, followed by 1000 rpm for 10 s) after which they were dried at  $T = 323 \text{ K}$  for at least 1 h on a hot plate. The thickness of the active layer was  $\sim 230 \text{ nm}$  as determined by profilometry. Al electrodes were deposited by thermal evaporation under high vacuum ( $p \approx 10^{-6} \text{ mbar}$ ) on top of the spin-coated films. All of the above-mentioned procedures, save for the cleaning of the substrates, were done in a glovebox under  $\text{N}_2$  atmosphere ( $[\text{O}_2] < 1 \text{ ppm}$  and  $[\text{H}_2\text{O}] < 1 \text{ ppm}$ ) or in an integrated thermal evaporator.

For the iTMCs-LECs, the devices were made as follows. The emitting complex,  $[\text{Ir}(\text{ppy})_2(\text{bpy})]^+ [\text{PF}_6]^-$ , was synthesized according to methods described previously.<sup>28</sup> Indium tin oxide ITO-coated glass plates were patterned by conventional photolithography ([www.narajosubstrates.com](http://www.narajosubstrates.com)). The substrates were cleaned by sonication in successively water-soap, water, and 2-propanol baths. After being

dried, the substrates were placed in an UV-ozone cleaner (Jelight 42–220) for 20 min. An 80 nm layer of PEDOT:PSS (CLEVIO P VP Al 4083, aqueous dispersion, 1.3–1.7% solid content, Heraeus) was spin-coated on the ITO glass substrate to improve the reproducibility of the devices and to prevent the formation of pinholes. A 100 nm transparent film of the emitting complex  $[\text{Ir}(\text{ppy})_2(\text{bpy})]^+[\text{PF}_6]^-$  was then spin-coated from 30 mg mL<sup>-1</sup> acetonitrile solution at 1000 rpm for 20 s. Unless stated otherwise, the ionic liquid (IL) 1-butyl-3-methylimidazolium hexafluorophosphate,  $[\text{BMIM}]^+[\text{PF}_6]^-$  (>98.5%, Sigma-Aldrich), was added in a 4:1 molar ratio (iTMC:IL). The thickness of the films was determined with an Ambios XP-1 profilometer. After the films were coated, the substrates were transferred to an inert atmosphere glovebox (<1 ppm O<sub>2</sub> and H<sub>2</sub>O, M. Braun). The Al electrode (70 nm) was thermally vacuum-evaporated using a shadow mask ( $<3 \times 10^{-6}$  mbar) with an Edwards Auto500 evaporator integrated in the glovebox. The area of the device was 6.5 mm<sup>2</sup>. The devices were not encapsulated and were characterized inside the glovebox.

For characterization of the p-LECs, a Keithley 2636a sourcemeter was used to drive the devices and measure the current. The brightness was measured with a luminance meter (LS-110 Konica-Minolta). A Solartron 1260 was used to perform complex admittance measurements on the LECs in the glovebox. Each point (from 10 MHz to 1 Hz) was measured during an integration time of 1 s. The rms value of the AC voltage was 0.01 V. The temperature of the device was controlled by use of a Peltier element, and the temperature was measured by a thermocouple.

For characterization of the iTMC-LECs, transients were measured by applying constant voltages and monitoring the current and luminance by a True Color Sensor MAZeT (MTCSiCT Sensor) using a Botest OLT OLED Lifetime-Test System. The conductance spectrum was determined by using a fast Fourier transform of the derivative of the transient current after setting a small step in the voltage (from 0 to -0.5 V to prevent carrier injection) by monitoring the current flow using a Keithley 2400 source meter via a Labview controlled custom-made protocol. The temperature of the device was controlled by use of a Peltier element, and the temperature was measured by a thermocouple.

Atomic force microscopy images of the active layer blends of both the polymer- and the iTMC-LEC are provided in the Supporting Information (Figures E.1 and 2).

## RESULTS AND DISCUSSION

The layouts of the iTMC- and polymer-based LECs as well as the structural formulas of the active layer constituents are shown in Figure 1a and b. Figure 2 shows the typical transient behaviors of the luminance, current, and efficacy in pristine iTMC- and p-LECs after application of 3.5 V at two different temperatures. In all measurements, the same is observed: current, luminance, and efficacy start to increase after which first the efficacy rolls off followed by the luminance. These typical transients can be rationalized by electrochemical doping of the active layer assisted by the mobile ions. Initially, upon application of a bias voltage, ions start moving and form EDLs at the electrode interfaces. This initiates injection of electrons and holes. Consequently, an electron–hole current arises that overtakes the ion current in magnitude. These electrons and holes recombine radiatively before reaching the other electrode. This explains the initial increase of current and luminance. The initial increase in efficacy results from the decreasing relative contribution of the ionic current with respect to the electronic current. Additionally, it may be related to a transition from unipolar to bipolar current due to more balanced carrier injection. After some time, the efficacy is observed to reach a maximum. The following decrease can be related to exciton quenching. This exciton quenching sets in after EDL formation when the semiconductor is being electrochemically doped: the

carrier density in the doped regions increases, and the n- and p-doped regions grow toward each other. The high polaron density in the doped regions close to the recombination region can cause significant exciton–polaron quenching.<sup>29</sup> Furthermore, the enhanced recombination current leads to an enhanced triplet exciton density in the iTMC-LEC. This is likely accompanied by triplet–triplet exciton annihilation.<sup>29</sup> After extended operation times, the current density reaches a maximum (not shown) followed by a decrease attributed to irreversible degeneration.<sup>17</sup>

For comparison, the transients in Figure 2a–d were all normalized and plotted in one graph, shown in Figure 3.

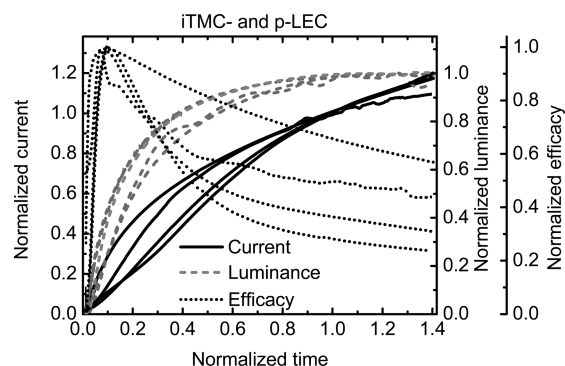


**Figure 3.** Normalized current, luminance, and efficacy transients of polymer and iTMC-LECs at two temperatures each and biased at 3.5 V.

Normalization of the transients was performed by division of the efficacy and luminance with their respective peak values. The time and current at which the luminance peaked was used to normalize these quantities, respectively. The good overlap of the transients in Figure 3 indicates that all four devices behave qualitatively the same, despite differences in semiconductor, ion-type, operational temperature, turn-on time, and magnitude of current, luminance, and efficacy. The invariance of the shape by temperature in particular indicates that a single process or property determines the turn-on behavior of these cells in this temperature range, most likely thermal activation of the “slow” ions. The fact that the use of different semiconductors and ions only leads to minor qualitative differences in the transients further proves that both types of devices operate according to the same operational model.<sup>8,9,11,15</sup> Processes such as ion dissociation and transport, exciton quenching, and electrochemical doping are (anticipated to be) active in both types of LECs. The large differences in the magnitude of the current, luminance, and efficacy can be related to differences in the type of emitting material and salt used as well as to the ratio in which they are mixed. For example, the Ir-iTMC is a phosphorescent emitter, whereas the PPV is a fluorescent emitter. Furthermore, the doping dependence of the carrier mobility is likely different, which may lead to differences in the thicknesses of the doped and intrinsic regions and as a consequence in the current density. The maximum efficacy of both types of LECs was however found to be independent of the operating temperature (see Supporting Information Figures A.2 and A.3).

Comparison of Figure 2a and b with, respectively, Figure 2c and d shows a strong temperature dependence of the turn-on time in both types of LECs: for the iTMC-LEC, the turn-on time changes from hours to tens of seconds by an increase of



the temperature from 27 to 60 °C (see Figure 2a and c). For the p-LEC, similar turn-on times are obtained in a different temperature range, −10 to 30 °C (see Figure 2b and d).

Similarly shaped turn-on transients were reported in other LECs, for example, in iTMC-LECs based on ruthenium with<sup>31</sup> and without<sup>32</sup> the addition of PEO. Polymer LECs without PEO have also been described; however, no constant voltage turn-on transients were reported.<sup>24,25</sup> Therefore, we prepared similar LECs comprising PPV and the salt tetrahexylammonium hexafluorophosphate. Again, similarly shaped turn-on transients were obtained despite a relatively large turn-on time in the order of hours (see Supporting Information Figure D.1), supporting our claim that the qualitative operation of semiconductor–electrolyte systems is universal despite potentially large differences in performance and response times.

The transients shown in Figure 2 originate from four different cells, which do show a variation in performance that is typical for LECs. To study the temperature dependence more carefully, more measurements were done on a single p- and iTMC-LEC. Again, the temperature had no effect on the shape of the current, luminance, and efficacy transients (see Supporting Information Figure A.1). When normalized, the transients at different temperatures collapse on top of each other. Therefore, the turn-on time can be quantified by an arbitrary point on the transients. Here, we take the time at which the efficacy reaches a maximum value. The invariance of the shape of the transients, the temperature independent peak efficacy, as well as additional PL quantum yield experiments on iTMC LECs (see Supporting Information Figure B.1) indicate that the EL efficacy is roughly temperature independent. In Figure 4, the natural logarithm of the inverse turn-on time was

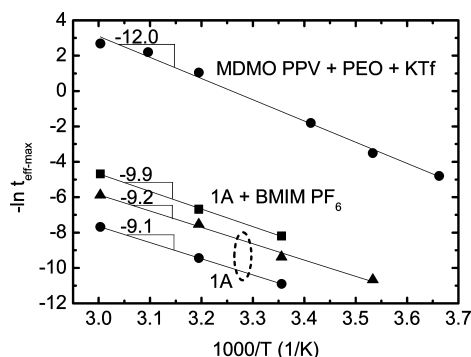


**Figure 4.** Arrhenius plots of the inverse maximum efficacy time iTMC-LECs with and without the ionic liquid BMIM PF<sub>6</sub> and an MDMO-PPV-based LEC. The activation energies determined from the fits are 1.03 and 0.78–0.85 eV for the p- and iTMC-LECs, respectively.

plotted against 1000/*T*. A linear decrease could be observed in both types of devices, hinting at an Arrhenius-type activation in this temperature range. The activation energy was determined to be ~0.8 eV for the iTMC-LEC and ~1.0 eV for the p-LEC. Arrhenius plots for iTMC-LECs without ionic liquid gave similar values for the activation energy (~0.8 eV) despite an order-of-magnitude slower response.

The transient behavior during turn-on is determined by the slowest charge carriers in the LECs: the ions. A way to study the transport of the ions is by looking at the ion conductivity at sub-bandgap voltages. For the p-LECs, the temperature dependence of the ion conductivity was measured by impedance spectroscopy.<sup>11</sup> For the iTMC-LECs, step response

experiments were performed because of the relatively slow ionic response.<sup>30</sup> Here, the voltage was stepped from 0.0 to −0.5 V. The relatively large size of the step was necessary to obtain a reasonable signal-to-noise ratio. The negative polarity of the voltage prevents any carrier injection from the electrodes at the used sub-bandgap voltages. More details on the actual method that was used can be found in Supporting Information section C.

Typical ion conductivity spectra at different temperatures of the iTMC- and p-LEC are shown in Figure 5a and b, respectively. All spectra contain a conductivity plateau that spans roughly 2 decades in the frequency range.<sup>11</sup> At higher frequencies, an increasing conductivity is observed that can be related to the response of the dielectric. At lower frequencies, a decreasing conductivity is observed related to EDL formation

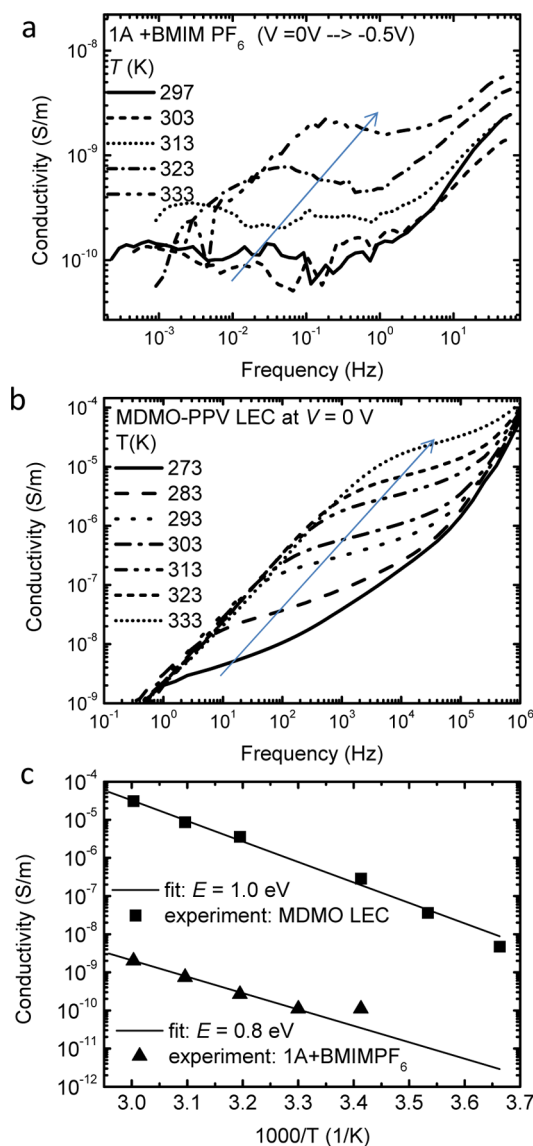


**Figure 5.** Conductivity spectra for (a) an iTMC LEC as determined by step response measurements from 0 V to −0.5 V and for (b) a polymer LEC as determined by impedance spectroscopy. (c) Fits of the ion conductivity by  $\sigma(T) = \sigma_0 e^{-E/kT}$  where the activation energy, *E*, was chosen equal to the activation energy determined in Figure 4. To fit the data, the values of  $\sigma_0$  used were  $1.6 \times 10^4$  and  $4.3 \times 10^{11}$  S m<sup>−1</sup> for the iTMC- and p-LEC, respectively.

that effectively decreases the electric field in the bulk. The minimal value of the measured conductance is  $\sim 10^{-10} \text{ S m}^{-1}$  below which leakage current starts to dominate the experiment. From the conductivity plateau, an estimate of the ion conductivity could be extracted as indicated by the arrows. These values are plotted in Figure 5c against  $1000/T$ . The linear decrease of the two semilog plots hints again at an Arrhenius-type activation. Note that the ion conductivity in the iTMC-LEC (see Figure 5a) at room temperature or below could not be determined because of the leakage current. Therefore, this data point was ignored in the fitting. The curves were fitted with the same activation energies as extracted from the activation in turn-on time in Figure 4. This shows that the ion conductivity and turn-on time have the same activation energy and thus are likely related. This strongly suggests that the turn-on time in both p- and iTMC-LECs is determined by the ionic conductivity, that is, the product of ion density and mobility. This process can be accelerated by, for example, (i) increasing the temperature, (ii) use of other (smaller) ions, (iii) addition of ion-solvating materials like PEO,<sup>1,24,31</sup> or (iv) increasing the applied bias voltage.

So far, the actual value of the determined activation energy has not been discussed. As ion conductivity is the product of ion density and mobility, its activation may also be split in these two components. The activation in ion density is then related to salt dissociation into ions, while the activation in ion mobility can be regarded as activation of viscosity. In polymer LECs, the equilibrium between the ion density  $n_i$  and salt density  $n_s$  can be described by the following expression:<sup>11,33</sup>

$$n_i^2 = n_s K e^{-E_b/kT} \quad (1)$$

Here,  $K$  is the mass action law constant.  $E_b$  is the binding energy that is generally estimated to lie between 0.2 and 0.6 eV.<sup>11,33</sup> For this range of binding energies at the used temperature range,  $n_s$  can be estimated to be much larger than  $n_i$ . As the sum of associated and dissociated salt is constant, the thermal activation of the ion density can be roughly described by  $n_i \approx \exp(E_b/2kT)$ . So effectively 0.1–0.3 eV of the 1.0 eV obtained in Figure 3d arises from the activation in mobile ion density. That means that the ion mobility has an activation energy of roughly 0.8 eV. The Arrhenius-type activation indicates that the ion conduction can be described by a simple ion hopping model. A barrier of  $\sim 0.8$  eV must be overcome by the ion to reach an adjacent site. This hopping is then facilitated by the motion of PEO chains.<sup>34</sup> In literature, activation energies of  $\sim 0.9$  eV are reported in high molecular weight PEO admixed with  $\text{LiCF}_3\text{SO}_3$ .<sup>35</sup> These values are comparable with the energies found in this work. In the iTMC-LECs, the salts are of a different nature as they consist of the large iTMC cation and a rather small anion. These ions are not very tightly bound, and therefore the dissociation energy is expected to be low. The activation energy observed for the iTMC-LECs may therefore be only related to the activation energy of the ionic mobility. The addition of ionic liquid only decreased the turn-on time as shown in Figure 4, whereas the activation energy remained more or less the same. This effect could originate from an increase in the prefactors of the mobility and carrier density. These prefactors may also explain why a higher activation energy is found in the polymer LEC, despite having a smaller turn-on time.

Mixed electronic and ionic conductive materials are used in a variety of systems and devices, such as organic photovoltaics,<sup>36,37</sup> and electrochemical,<sup>38</sup> biological, and organic

bioelectronic<sup>39,40</sup> systems and devices. Therefore, the results obtained here can be of use to establish the dynamic operation of these devices.

## CONCLUSIONS

Despite large quantitative differences, the transient behavior of iTMC- and p-LECs after switch-on is shown to be qualitatively equal. This further confirms the identical operational behavior in both types of LECs. The qualitative transients are independent of semiconductor- and ion-type and also of the temperature. The thermal activation of both the turn-on time and the ion conductivity in the unbiased state was found to be proportional and could be described by Arrhenius-type activation with an activation energy of  $\sim 0.8$ –1.0 eV. These results clearly demonstrate that p-LECs and iTMC-LECs are really behaving as one class of device.

## ASSOCIATED CONTENT

### Supporting Information

Non-normalized transients, temperature-dependent quantum yield in Ir-iTMC-LECs, details regarding the step response method to determine the ionic conductivity, turn-on transients of a polymer LEC without PEO, and AFM images of the active layer blends. This material is available free of charge via the Internet at <http://pubs.acs.org>.

## AUTHOR INFORMATION

### Corresponding Author

[m.kemerink@tue.nl](mailto:m.kemerink@tue.nl); [henk.bolink@uv.es](mailto:henk.bolink@uv.es)

### Notes

The authors declare no competing financial interest.

## ACKNOWLEDGMENTS

We are grateful to Edwin Constable and Gabriel Schneider of the University of Basel for supplying the iridium complex. S.v.R. and M.K. acknowledge financial support from the Dutch program NanoNextNL. T.A., D.T., and H.J.B. acknowledge financial support from the European Community's Seventh Framework Program under grant agreement no. FP7-ICT-248043 ([www.CELLO-project.eu](http://www.CELLO-project.eu)), the Spanish Ministry of Economy and Competitiveness (MINECO) (MAT2011-24594), and the Generalitat Valenciana (Prometeo/2012/053). D.T. acknowledges MECO (Spanish Ministry of Education, Culture, and Sport) for an FPU grant.

## REFERENCES

- (1) Pei, Q. B.; Yu, G.; Zhang, C.; Yang, Y.; Heeger, A. J. *Science* **1995**, 269, 1086.
- (2) Lee, J. K.; Yoo, D. S.; Handy, E. S.; Rubner, M. F. *Appl. Phys. Lett.* **1996**, 69, 1686.
- (3) Maness, K. M.; Terrill, R. H.; Meyer, T. J.; Murray, R. W.; Wightman, R. M. *J. Am. Chem. Soc.* **1996**, 118, 10609.
- (4) Sun, Q.; Li, Y.; Pei, Q. B. *J. Disp. Technol.* **2007**, 3, 211.
- (5) Costa, R. D.; Orti, E.; Bolink, H. J.; Monti, F.; Accorsi, G.; Armaroli, N. *Angew. Chem., Int. Ed.* **2012**, 51, 8178.
- (6) deMello, J. C.; Tessler, N.; Graham, S. C.; Friend, R. H. *Phys. Rev. B* **1998**, 57, 12951.
- (7) Slinker, J. D.; DeFranco, J. A.; Jaquith, M. J.; Silveira, W. R.; Zhong, Y. W.; Moran-Mirabal, J. M.; Craighead, H. G.; Abruna, H. D.; Marohn, J. A.; Malliaras, G. G. *Nat. Mater.* **2007**, 6, 894.
- (8) Matyba, P.; Maturova, K.; Kemerink, M.; Robinson, N. D.; Edman, L. *Nat. Mater.* **2009**, 8, 672.
- (9) Lenes, M.; Garcia-Belmonte, G.; Tordera, D.; Pertegas, A.; Bisquert, J.; Bolink, H. J. *Adv. Funct. Mater.* **2011**, 21, 1581.

- (10) van Reenen, S.; Matyba, P.; Dzwilewski, A.; Janssen, R. A. J.; Edman, L.; Kemerink, M. *J. Am. Chem. Soc.* **2010**, *132*, 13776.
- (11) van Reenen, S.; Janssen, R. A. J.; Kemerink, M. *Adv. Funct. Mater.* **2012**, *22*, 4547.
- (12) Meier, S. B.; Hartmann, D.; Tordera, D.; Bolink, H. J.; Winnacker, A.; Sarfert, W. *Phys. Chem. Chem. Phys.* **2012**, *14*, 10886.
- (13) Munar, A.; Sandstrom, A.; Tang, S.; Edman, L. *Adv. Funct. Mater.* **2012**, *22*, 1511.
- (14) Mills, T. J.; Lonergan, M. C. *Phys. Rev. B* **2012**, 85.
- (15) Meier, S. B.; Van Reenen, S.; Lefevre, B.; Hartmann, D.; Bolink, H. J.; Winnacker, A.; Sarfert, W.; Kemerink, M., unpublished.
- (16) Rodovsky, D. B.; Reid, O. G.; Pingree, S. C.; Ginger, D. S. *ACS Nano* **2010**, *4*, 2673.
- (17) Asadpoordarvish, A.; Sandstrom, A.; Tang, S.; Granstrom, J.; Edman, L. *Appl. Phys. Lett.* **2012**, 100.
- (18) Fang, J. F.; Matyba, P.; Edman, L. *Adv. Funct. Mater.* **2009**, *19*, 2671.
- (19) Edman, L.; Tang, S. *J. Phys. Chem. Lett.* **2010**, *1*, 2727.
- (20) Sandstrom, A.; Matyba, P.; Edman, L. *Appl. Phys. Lett.* **2010**, 96.
- (21) Yu, Z.; Wang, M.; Lei, G.; Liu, J.; Li, L.; Pei, Q. *J. Phys. Chem. Lett.* **2011**, *2*, 6.
- (22) Tordera, D.; Meier, S.; Lenes, M.; Costa, R. D.; Orti, E.; Sarfert, W.; Bolink, H. J. *Adv. Mater.* **2012**, *24*, 897.
- (23) Tordera, D.; Delgado, M.; Orti, E.; Bolink, H. J.; Frey, J.; Nazeeruddin, M. K.; Baranoff, E. *Chem. Mater.* **2012**, *24*, 1896.
- (24) Shao, Y.; Bazan, G. C.; Heeger, A. J. *Adv. Mater.* **2007**, *19*, 365.
- (25) Gautier, B.; Gao, J. *Appl. Phys. Lett.* **2012**, 101.
- (26) Hoven, C. V.; Wang, H. P.; Elbing, M.; Garner, L.; Winkelhaus, D.; Bazan, G. C. *Nat. Mater.* **2010**, *9*, 249.
- (27) Kosilkin, I. V.; Martens, M. S.; Murphy, M. P.; Leger, J. M. *Chem. Mater.* **2010**, *22*, 4838.
- (28) Costa, R. D.; Orti, E.; Bolink, H. J.; Graber, S.; Schaffner, S.; Neuburger, M.; Housecroft, C. E.; Constable, E. C. *Adv. Funct. Mater.* **2009**, *19*, 3456.
- (29) Baldo, M. A.; Holmes, R. J.; Forrest, S. R. *Phys. Rev. B* **2002**, *66*.
- (30) Macdonald, D. D. *Electrochim. Acta* **2006**, *51*, 1376.
- (31) Lyons, C. H.; Abbas, E. D.; Lee, J. K.; Rubner, M. F. *J. Am. Chem. Soc.* **1998**, *120*, 12100.
- (32) Bolink, H. J.; Cappelli, L.; Coronado, E.; Grätzel, M.; Nazeeruddin, M. K. *J. Am. Chem. Soc.* **2006**, *128*, 46.
- (33) Smith, D. L. *J. Appl. Phys.* **1997**, *81*, 2869.
- (34) Mendolia, M. S.; Farrington, G. C. *Chem. Mater.* **1993**, *5*, 174.
- (35) Leo, C. J.; Rao, G. V. S.; Chowdari, B. V. R. *Solid State Ionics* **2002**, *148*, 159.
- (36) Hany, R.; Fan, B.; Arajio de Castro, F.; Heier, J.; Kylberg; Nuesch, F. *Prog. Photovolt. Res. Appl.* **2011**, *19*, 851.
- (37) Su, M.-S.; Su, H.-C.; Kuo, C.-Y.; Zhou, Y.-R.; Wei, K.-H. *J. Mater. Chem.* **2011**, *21*, 6217.
- (38) Kim, S.; Yamaguchi, S.; Elliot, J. A. *MRS Bull.* **2009**, *34*, 900.
- (39) Owens, R. M.; Malliaras, G. G. *MRS Bull.* **2010**, *35*, 449.
- (40) Berggren, M.; Richter-Dahlfors, A. *Adv. Mater.* **2007**, *19*, 3201.